

## Interlayer-coupling magnetism and electronic structure of Fe/Cr(001) superlattices

Jian-hua Xu

*Department of Physics and Astronomy, Northwestern University, Evanston, Illinois 60208-3112*

A. J. Freeman

*Department of Physics and Astronomy, Northwestern University, Evanston, Illinois 60208-3112  
and Materials Science Division, Argonne National Laboratory, Argonne, Illinois 60439*

(Received 24 April 1992; revised manuscript received 13 July 1992)

The electronic structure and magnetism of  $\text{Fe}_m/\text{Cr}_n(001)$  superlattices with varying layer thickness ( $m = 1, 3$  and  $n = 1, 3, 5, 7$ ) were studied using the all-electron total-energy self-consistent linear muffin-tin orbital method based on the local-density approximation. Similar to the Fe/Cr(110) superlattices, (i) there is a strong hybridization between Cr  $d$  and Fe  $d$  states; (ii) the absolute values of the magnetic moments of the Fe layers are not significantly modified by the intervening Cr layers. The small moment found on the interfacial Cr atoms is aligned antiparallel for 3 Fe layers and parallel for monolayer Fe to the nearest-neighbor Fe moments in the  $\text{Fe}_m/\text{Cr}_n(001)$  superlattices, respectively. For the former case the ferromagnetic alignment for the two consecutive Fe layers separated by Cr layers dominates over the antiferromagnetic alignment, whereas a crossover is seen when the number of Cr layers is increased to 5 (or perhaps 3) layers in between a single Fe layer, i.e., a (slightly) lower total energy for the antiferromagnetic state with respect to the ferromagnetic state.

### I. INTRODUCTION

Baibich *et al.*<sup>1</sup> reported for Fe/Cr(001) superlattices with increasing Cr thickness below  $\sim 30$  Å that (i) the magnetization becomes harder to saturate, (ii) the remanent magnetization decreases to almost zero, (iii) the magnetoresistance is reduced by about a factor of 2 in high magnetic fields. This behavior has been attributed to an antiferromagnetic (AFM) coupling between the two consecutive Fe layers separated by Cr layers. As a result, considerable interest has arisen in studying their various physical properties and in attempting to probe the underlying physical mechanism responsible for the magnetic couplings in  $\text{Fe}_m/\text{Cr}_n$  superlattices.<sup>2-10</sup> Interestingly, the prediction of a crossover to AFM coupling with increasing thickness was actually first predicted by Jarlborg and Freeman<sup>11</sup> in their pioneering studies on  $\text{Ni}_m/\text{Cu}_n$  superlattices. In these investigations, they noted that the small  $s, p$  moments, which may determine the long-range spin coupling (in the case for Ni films across the Cu layers), vary commensurately with the lattice modulation for  $\text{Ni}_6/\text{Cu}_6$ , while they change their sign and amplitude irregularly for  $\text{Ni}_3/\text{Cu}_3$ . When coupled with information about the Ni majority spin Fermi surface (FS) looking very similar to that of Cu and the nesting vectors of Ni majority and minority spin FS differing by  $\frac{1}{6}$  of the distance between  $\Gamma$  and  $K$ , they predicted a possible AFM coupling in the Ni/Cu superlattices, when the composition modulation period is about six monolayers along the (111) direction. Some evidence for AFM coupling in Ni/Cu was reported by Flevaris.<sup>12</sup> Among the various experiments performed, two are especially worthy of mention: (i) neutron diffraction<sup>4</sup> provided clear evidence for the AFM spin arrangement; (ii) the magnetoresis-

tance<sup>5</sup> exhibits a long-range oscillatory behavior as a function of the Cr (Ru) layer thickness with a period 18–20 Å in transition metal Fe/Cr and Co/Cr (Co/Ru) multilayers.

To understand the physical origin of the AFM coupling between two consecutive Fe layers separated by Cr layers, a number of studies (including first-principle total-energy local-density calculations)<sup>6-9</sup> have been carried out on the Fe/Cr(001) superlattices. Using the augmented spherical wave (ASW) method, Levy *et al.*<sup>6</sup> studied the electronic structure, interlayer magnetic coupling, and magnetoresistance of the  $\text{Fe}_m/\text{Cr}_n(001)$  ( $m = 3, 4$  and  $n = 3, 4, 5$ ) superlattices. Their total-energy results showed that the AFM coupling for the Fe layers can be stabilized except in the  $m/n = 3/3$  case for which the ferromagnetic configuration is favored. Similar moments (or moment distributions) of the  $\text{Fe}_m/\text{Cr}_n(001)$  superlattices were also obtained using real-space approaches [the self-consistent tight-binding (TB) method<sup>7</sup> and the TB method combined with the recursion method<sup>8</sup>]. Recently, Herman, Sticht, and Schilfgaard<sup>9</sup> found an alternating sign change in the total-energy difference between the AFM and the ferromagnetic (FM) configurations depending on the thickness (or number) of Cr layers. They noted that their result is inconsistent with experiment.<sup>1,5</sup> For reconciling the calculated results with experiment they presumed that interfacial roughness and impurities effects may play a significant role. Previously,<sup>13</sup> we studied the electronic structures and the (ferro)-magnetism of the Fe/Cr(110) superlattices using the self-consistent linear muffin-tin orbit (LMTO) method with the combined correction term,<sup>14</sup> and found that in agreement with experiment,<sup>15</sup> the magnetic moments of the Fe layers are not substantially affected by the Cr layers, and have almost the same magnitude as in bulk bcc Fe, even

in the case of an intervening Fe monolayer. Only a small moment ( $\leq 0.4\mu_B$ ) was found for the Cr layers, and always aligned antiparallel to the nearest neighbor (nn) Fe moments.

In this work, the electronic structures of bcc  $\text{Fe}_m/\text{Cr}_n(001)$  ( $m=1,3$  and  $n=1,3,5,7$ ) superlattices were investigated using the self-consistent total-energy LMTO method with the combined correction term. We determined the stable interlayer magnetic coupling (having AFM or FM character) between the two Fe layers separated by Cr layers simply by comparing their total energies. Our total energy results showed that, except in the interfacial region, the moments of the Fe and Cr atoms prefer to keep their bulk form, as a result of the competition between the nn Cr-Cr and Fe-Fe interactions. For the  $\text{Fe}_m/\text{Cr}_n(001)$  systems containing three (or perhaps more) Fe layers, the FM ordering dominates over the AFM state, whereas for the  $\text{Fe}_m/\text{Cr}_n(001)$  systems containing a single Fe layer (i.e.,  $m=1$ ) the AFM interactions may slightly exceed the FM interactions. Thus, it seems that the bulk effect dominates over the interface effect.

## II. METHODOLOGY

A common bcc-based structure consisting of  $m$  Fe layers and  $n$  Cr layers stacked along the (001) direction was constructed to simulate a  $\text{Fe}_m/\text{Cr}_n(001)$  superlattice (cf. Fig. 1). A weighted average of the lattice constants of the constituents is assumed (i.e., Vegard's law<sup>16</sup> holds), because both Fe and Cr have the same bcc structure and approximately the same lattice constant (2.87 Å and 2.88 Å for Fe and Cr, respectively<sup>17</sup>); the same Wigner-Seitz (WS) sphere radius is assumed for all atoms. In order for both paramagnetic and magnetic (including both AFM and FM) calculations to have the same number of sampling  $k$  points in the irreducible wedge of the Brillouin zone (IBZ), we take the double primitive cell as a unit cell; therefore, each unit cell contains two formula units. In this way, a cancellation of errors can be invoked to assure greater accuracy. The basis set includes  $s, p$ , and  $d$  orbitals. The von Barth-Hedin formula<sup>18</sup> for the exchange and correlation potential is adopted. The self-consistent calculations were performed at an arbitrarily chosen 30  $k$  points within the  $\frac{1}{16}$  wedge of the IBZ. In general, the calculated moments and the absolute value of the total energy increases gradually with increasing number of sampling  $k$  points. In the  $\text{Fe}_m/\text{Cr}_n$  ( $m=n=3$ ) case, we studied the dependence of the total energy and the moments on the number of sampling  $k$  points ( $= 30, 60, \text{ and } 90$ ) within the IBZ; and, as was also shown in Ref. 19, the use of 30  $k$  points in the IBZ allows one to obtain better than 1% accuracy in the converged moments. The total energy is converged to better than  $10^{-2}$  mRy/unit cell.

Each layer in the unit cell contains only one atom, and moments within a layer are assumed to be parallel. In the starting configuration, the moments were set equal to zero on the Cr sites, and initial fields were set up on the Fe sites that permit parallel (ferromagnetic) or antiparallel (antiferromagnetic) spin alignments for the two con-

secutive Fe layers. After a few iterations the field was removed, and all the magnetic moments were allowed to relax and be determined self-consistently. One remark needs to be made at this point, we should not mix up the FM and AFM configurations, which stand for the magnetic moment alignment between the two consecutive Fe slabs separated by Cr layers, with the ferromagnetic and the antiferromagnetic interlayer coupling between the Fe and Cr atoms across the interface layer.

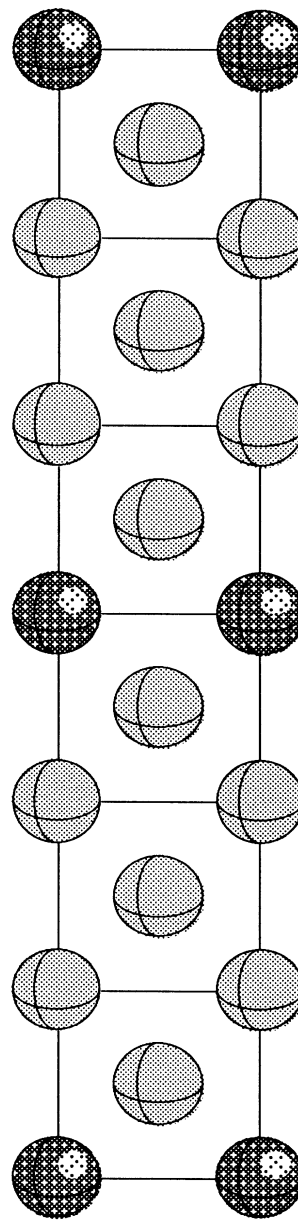


FIG. 1. A sideview of the unit cell for the  $\text{Fe}_m/\text{Cr}_n(001)$  ( $m=1, n=5$ ) superlattice. Dark and dotted circles denote the Fe and Cr atoms, respectively.

### III. RESULTS AND DISCUSSION

The calculated magnetic moments within each WS sphere for the  $\text{Fe}_m/\text{Cr}_n(001)$  superlattices are listed in Table I. The overall absolute values of the magnetic moments of the Fe layers are not significantly modified by the presence of the Cr layers. Somewhat different magnetic moments on the Fe layers are seen compared with those of the Fe/Cr(110) superlattices.<sup>13</sup> The moment on the center (or bulklike) Fe layer ( $2.57\mu_B$ ) is strongly enhanced compared with that ( $2.20\mu_B$ ) of pure bulk bcc Fe, and also higher than that ( $\sim 2.40\mu_B$ ) of the center Fe layers in the Fe/Cr(110) superlattices. On the other hand, the moments ( $1.6\text{--}2.07\mu_B$ ) on the interfacial Fe layers are generally reduced with respect to those of the pure bcc Fe and those ( $2.1\text{--}2.2\mu_B$ ) of the interfacial layers in the  $\text{Fe}_m/\text{Cr}_n(110)$  superlattices. (A strong hybridization between the Fe-*d* and Cr-*d* states is thought to be responsible for the moment reduction;<sup>8</sup> the interlayer coupling will be discussed later in view of the density of states). However, similar to the  $\text{Fe}_m/\text{Cr}_n(110)$  case, the magnetic moments on the Cr sites are generally much smaller than those of the pure bcc Cr spin density wave (SDW) value ( $0.60\mu_B$ ),<sup>20</sup> except for  $\text{Fe}_m/\text{Cr}_n(001)$  ( $m=3$ ) in the FM configuration case, which has a slightly enhanced moment ( $\leq 0.7\mu_B$ ) compared to that of the bcc Cr SDW value.

In the  $\text{Fe}_m/\text{Cr}_n(001)$ , the magnetization on the adjacent Fe sites can be viewed as a strong perturbation field for the Cr moments; as a result, the variation (enhancement or frustration) of the moments on the Cr sites is thought to depend strongly on the Fe moment ordering (or alignment) and on the coupling between Fe and Cr layers. For instance, when a magnetic arrangement on two consecutive Fe layers separated by Cr layers is compatible with the development of the SDW on the Cr sites, the magnetic moments on the Cr sites are close to their bcc SDW value<sup>6</sup> (i.e., the  $\text{Fe}_m/\text{Cr}_n(001)$  ( $m=3$ ) in the FM configuration case [cf. Figs. 2(b) and 2(c) in the FM configuration]). Otherwise the Cr moments are suppressed drastically to far below  $0.6\mu_B$  [cf. Fig. 1, Figs. 2(b), and 2(c) in AFM configuration].

In general, our calculated magnetic moment distribution for the  $\text{Fe}_m/\text{Cr}_n(001)$  ( $m=3$ ) superlattice agree quantitatively with those of Ref. 6 obtained by the ASW

method (cf. Table I). The Cr moments alternate direction from layer to layer, and an antiferromagnetic coupling between Fe and Cr at the interfacial layer is seen [cf. Figs. 2(b) and 2(c)]. By contrast, for the  $\text{Fe}_m/\text{Cr}_n(001)$  ( $m=1$ ) case, the magnetic moments of the interfacial Cr atoms are often aligned parallel to the moments of the neighboring Fe atoms (i.e., a ferromagnetic coupling across the interface layer) [cf. Fig. 2(a)], which is also contrary to the case of Fe/Cr(110). Note that a ferromagnetic interlayer coupling between Co and Cr atoms across the interface layer was also found in the  $\text{Co}_m/\text{Cr}_n$  ( $m=1$ ) (001) superlattice.<sup>19</sup>

In brief, for the  $\text{Fe}_m/\text{Cr}_n(001)$  superlattices our calculated moment distribution showed that (i) the moments in the Fe region always align parallel whereas those in the Cr region align antiparallel, and (ii) the character of the interfacial coupling between Fe and Cr atoms varies from ferromagnetic coupling for the  $\text{Fe}_m/\text{Cr}_n(001)$  ( $m=1$ ) superlattices to antiferromagnetic coupling for the  $\text{Fe}_m/\text{Cr}_n(001)$  ( $m=3$ ) superlattices, which implies significant Fe second-nearest-neighbor interactions.

Table II shows the total-energy difference between the AFM and FM configurations. Note that for all  $\text{Fe}_m/\text{Cr}_n(001)$  superlattices containing  $m=3$  layers of Fe, our calculated  $\Delta E$  ( $\sim +3\text{--}4$  mRy/unit cell) always shows a positive value, that is qualitatively consistent with Ref. 9 ( $\sim +13$  mRy/unit cell); the quantitative difference between Ref. 9 and our result is thought to be caused by the different number of Fe layers adopted in the calculations. A positive  $\Delta E$  means that the FM configuration is energetically favored with respect to the AFM configuration. This is obviously contrary to the results of Ref. 6 that the AFM state is stable over the FM state for  $m/n=3/5$  or  $4/4$ . The difference between Ref. 6 and ours may be attributed to the different convergence in the total energy (their  $10^{-1}$  mRy vs our  $10^{-2}\text{--}10^{-3}$  mRy). The AFM calculation needs to be viewed cautiously due to its extremely slow convergence; for the  $m=1$  superlattices, we did find a (slightly) lower total energy for AFM compared with FM upon increasing the number of Cr layers to five (or perhaps three) (cf. Table II).

Table III exhibits the dependence of the total-energy difference,  $\Delta E$ , between the FM and AFM configurations on the number of *k* points sampled for the  $m=n=3$

TABLE I. Calculated magnetic moments (in Bohr magnetons) for the  $\text{Fe}_m/\text{Cr}_n(001)$  superlattices with  $m=1,3$  and  $n=1,3,5,7$ . Superscripts *i* and *b* stand for interface and bulklike atoms.

			Fe <sup><i>i</i></sup>	Fe <sup><i>b</i></sup>	Cr <sup><i>i</i></sup>	Cr <sup><i>b</i></sup>
This work	1/ <i>n</i>	(FM)	1.6–1.8		$\leq 0.2$	$\leq 0.25$
		(AFM)	1.6–1.8		$\leq 0.26$	$\leq 0.1$
	3/ <i>n</i>	(FM)	1.8–2.07	2.57	$\leq 0.7$	$\leq 0.6$
		(AFM)	1.8–2.07	2.57	$\leq 0.37$	$\leq 0.2$
a		1.8	2.5	$\leq 0.6$	$\leq 0.45$	
b	(110)	(FM)	2.1–2.2	2.4	$\leq 0.4$	$\leq 0.4$

<sup>a</sup>Reference 6.

<sup>b</sup>Reference 13.

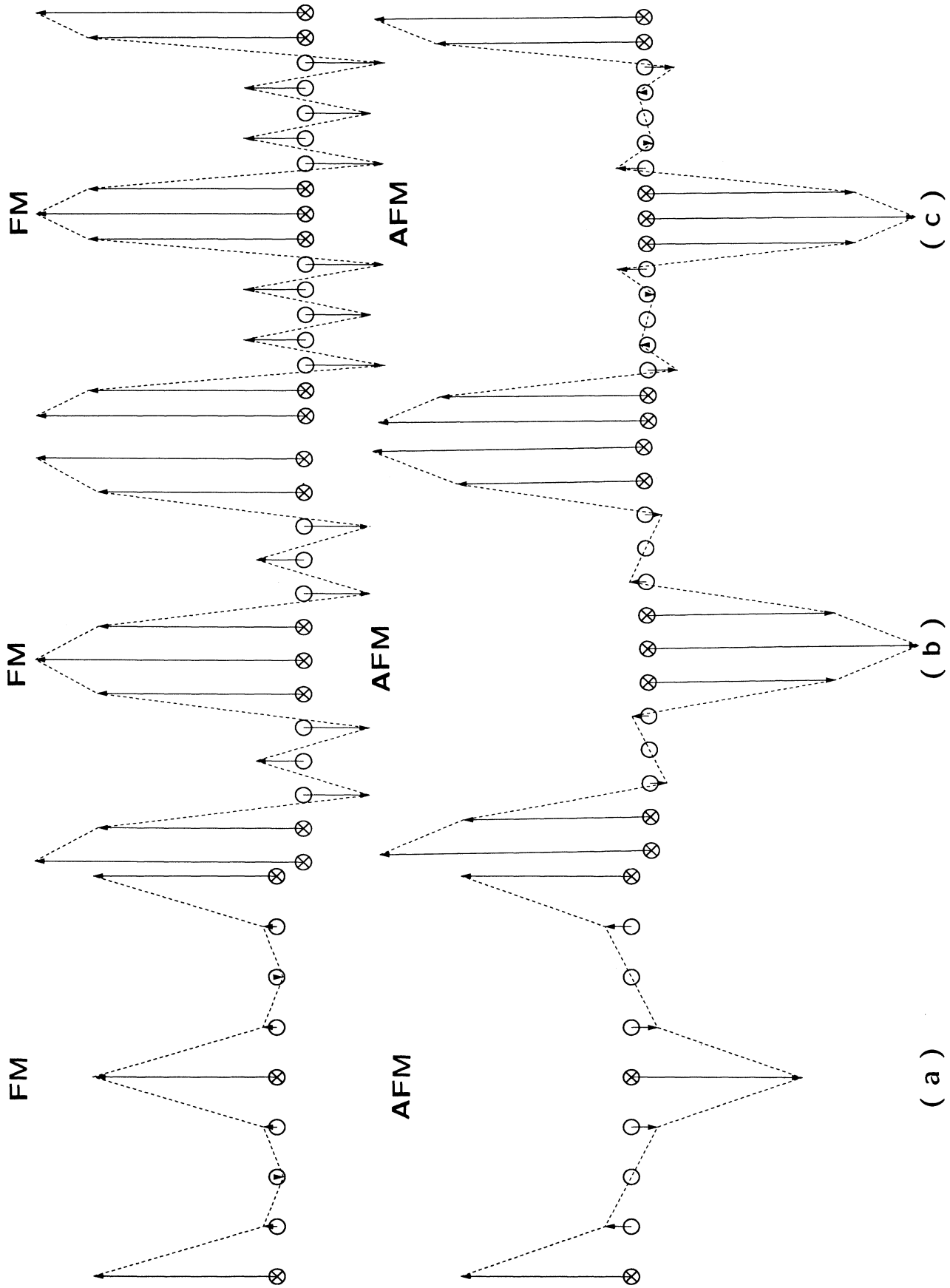


FIG. 2. Moment distribution for the  $\text{Fe}_m/\text{Cr}_n$  (001) superlattices with  $m/n$ : (a) 1/3, (b) 3/3, and (c) 3/5. FM and AFM stand for ferromagnetic and antiferromagnetic alignment between the two consecutive Fe slabs separated by Cr layers. Crossed and open circles denote the Fe and Cr atoms, respectively. The dotted line is only as a guide for the eye.

TABLE II. Total energy  $E$  (in mRy/unit cell) for  $\text{Fe}_m/\text{Cr}_n$  (001) superlattices, using 30  $k$  points within the IBZ ( $m$  and  $n$  stand for the number of layers).  $E_{\text{para-}}$  is taken as energy zero.

$m/n$	$E_{\text{ferro-}}$	$E_{\text{antiferro-}}$	$\Delta E$	Ref. 6
1/1	$\sim -26^a$	-11.9	$\sim 14$	
1/3	-11.0	-11.7	-0.7	
1/5	-13.4	-15.5	-2.1	
3/3	-162.2	-159.0	3.2	2.5
3/5	-180.0	-176.4	3.6	-22
3/7	-178.2	-174.4	3.8	

<sup>a</sup>Obtained using the primitive unit cell.

case. The absolute value of  $\Delta E$  shows a slight increase (from 3 to 4 mRy) with increase of the number of  $k$  points, but qualitatively the results remain the same, i.e., the FM configuration is favored over the AFM one.

In order to understand the magnetic behavior of the Fe and Cr atoms in the  $\text{Fe}_m/\text{Cr}_n$ (001) superlattices we inspect the density of states (DOS) in their paramagnetic states. It is expected that the fundamental features of the total DOS for  $\text{Fe}_m/\text{Cr}_n$ (001) (cf. Fig. 3), similar to that of Fe/Cr(110), will resemble those of their constituents (i.e.,

TABLE III. Total-energy difference  $\Delta E$  (in mRy/unit-cell) vs the number of  $k$  points within IBZ for  $\text{Fe}_m/\text{Cr}_n$ (001) ( $m = n = 3$ ) superlattices ( $m$  and  $n$  stand for the number of layers).

Num. of $k$	$\Delta E$
30	3.2
60	3.7
90	4.3

typical bcc Fe or Cr-like DOS). There are three main features located at  $-4.0$ ,  $-2.0$ , and from  $0.0$  to approximately  $1.0$  eV, respectively. The partial  $d$  DOS for  $\text{Fe}_m/\text{Cr}_n$ (001) with layer thickness  $m = 1, 3$   $n = 3.5$  are shown in Fig. 4. As a characteristic feature, a pervasively strong hybridization between Fe  $d$  and Cr  $d$  states in the whole energy region from the bottom of the band up to high above  $E_f$  is seen. As stated above, the reduction of the interfacelike  $\text{Fe}^i$  and  $\text{Cr}^i$  momenta are thought to be related to the strong  $d$ - $d$  hybridization between the Fe  $d$  and Cr  $d$  states.<sup>8</sup> Furthermore, the character of the  $d$ - $d$  hybridization apparently also governs the character of the interlayer coupling between  $\text{Fe}^i$  and  $\text{Cr}^i$  atoms. For

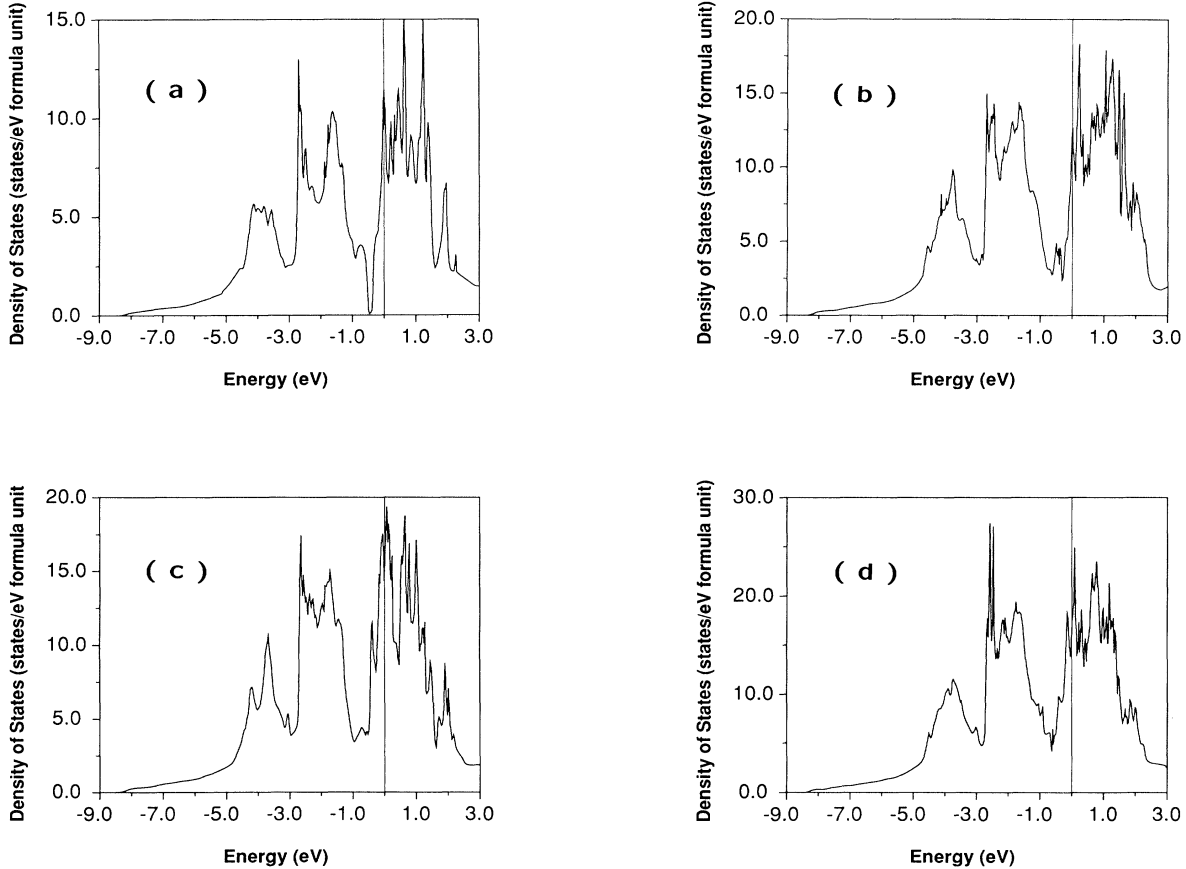


FIG. 3. Total density of states (paramagnetic state) for the  $\text{Fe}_m/\text{Cr}_n$ (001) superlattices with  $m/n$ : (a) 1/3, (b) 1/5, (c) 3/3, and (d) 3/5.

instance, for the  $m = 1$  case, there is an extremely strong  $d$ - $d$  hybridization at  $E_F$  [cf. Figs. 4(a) and 4(b)]; the Fermi energy located on the peak of both Fe  $d$  and Cr  $d$  states indicates that both Fe and Cr dominate its magnetism; the result is a ferromagnetic coupling across the interface region—as is seen in the spin-dependent density of states shown in Fig. 5 for the  $\text{Fe}_1/\text{Cr}_3$ , which compares both the FM and AFM configurations. Note that a ferromagnetic coupling between the  $\text{Fe}^i d$  and  $\text{Cr}^i d$  interface states is shown in Figs. 5(a) and 5(b) for the FM configurations and in Figs. 5(d) and 5(e) for the AFM configuration, respectively.

By contrast, for the  $m = 3$  superlattices, there is only a moderate  $d$ - $d$  hybridization at  $E_F$ ; the Fermi energy mainly lies on the peak of the Fe  $d$  states [cf. Figs. 4(c) and 4(d)], which implies that the magnetism is basically dominated by the Fe atoms, and it exhibits an antiferromagnetic coupling at the interface region. This is indeed the case; an antiferromagnetic coupling between the  $\text{Fe}^i d$  and  $\text{Cr}^i d$  interface states is seen for the  $\text{Fe}_3/\text{Cr}_3$  superlattice in both the FM [cf. Figs. 6(b) and 6(c)] and AFM [cf. Figs. 6(f) and 6(g)] configurations. This is also the case for the Fe/Cr (110) superlattices, where it has been known that the magnetic instability is basically due to the Fe atoms [cf. Fig. 2(a) in Ref. 13], even in the case of

monolayer Fe in the Fe/Cr(110) system. Moreover, as is well known, the Fe and Cr moments in their own pure bulk states (i.e., the bcc structure) strongly prefer to align parallel and antiparallel to their first nn, respectively. For the  $\text{Fe}_m/\text{Cr}_n(001)$  systems, as stated above, except in the interfacial region the Fe and Cr moments prefer to stay in their bulk form, i.e., the Fe region is always in the ferromagnetic state whereas the Cr region is in the antiferromagnetic state (cf. Fig. 2). Therefore, our total-energy results seem to show that as a result of the competition between the nn Cr-Cr and Fe-Fe interactions, for the  $\text{Fe}_m/\text{Cr}_n(001)$  systems containing three (or perhaps more) Fe layers energetically FM dominates over AFM. On the other hand, for  $\text{Fe}_m/\text{Cr}_n(001)$  containing a single Fe layer (i.e.,  $m = 1$ ) the AFM interactions may slightly surpass the FM interactions; it seems that the bulk effect dominates over the interface effect.

Finally, the difference in the magnetism and the electronic structure between the single layer ( $m = 1$ ) and the three layers ( $m = 3$ ) Fe sandwiched in the  $\text{Fe}_m/\text{Cr}_n(001)$  superlattices can be traced back to the difference of their first nn environment. For instance, all single Fe layer cases, contain only the interfacelike Fe layers (denoted as  $\text{Fe}^i$ ). Each  $\text{Fe}^i$  atom is always surrounded by eight Cr interfacelike (denoted as  $\text{Cr}^i$ ) atoms as its first nn. This

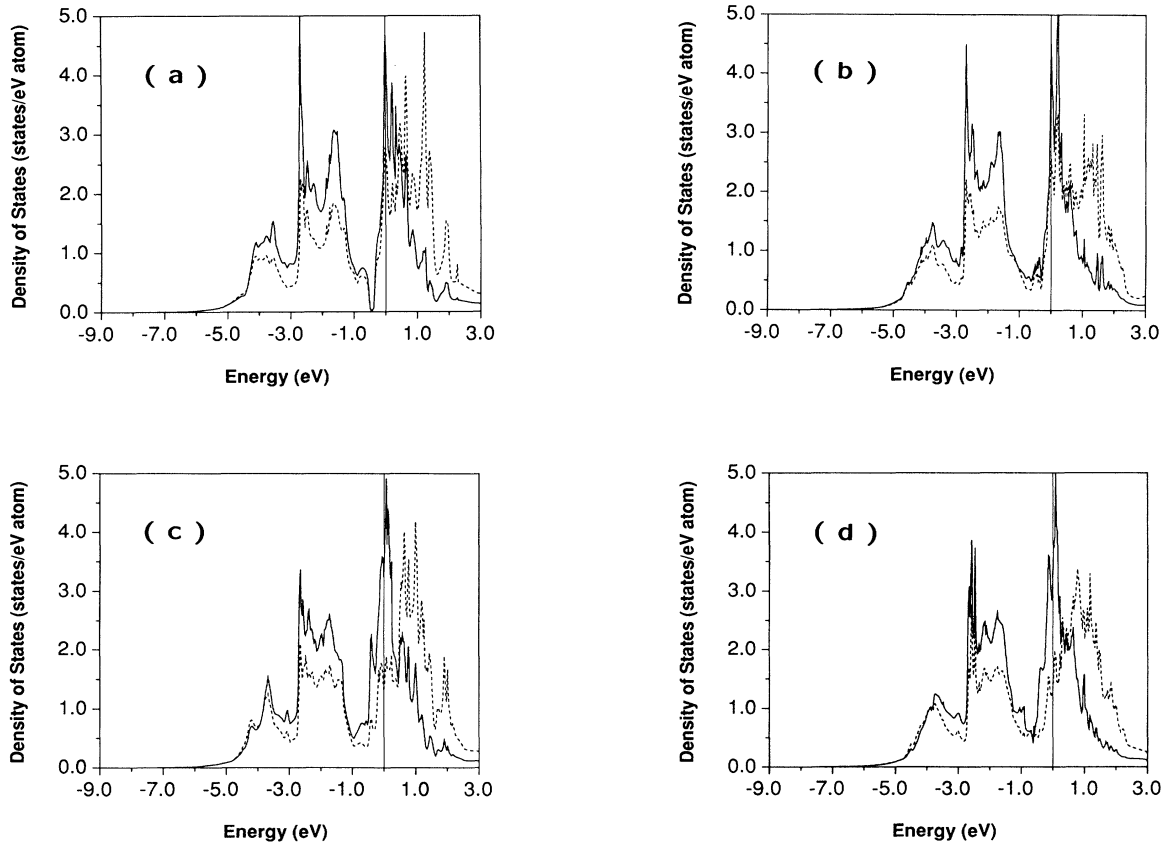


FIG. 4. Partial density of states (paramagnetic state) for the  $\text{Fe}_m/\text{Cr}_n(001)$  superlattices with  $m/n$ : (a) 1/3, (b) 1/5, (c) 3/3, and (d) 3/5. Solid and dotted lines denote  $\text{Fe}^i d$  and  $\text{Cr}^i d$  states, respectively. The superscript  $i$  stands for interfacelike atoms.

leads to an extremely strong hybridization between Fe  $d$  and Cr  $d$  states [cf Figs. 4(a) and 4(b)]. On the other hand, for the  $m=3$  Fe layer case, the first nn consists of half interfacelike Cr<sup>*i*</sup> and half bulklike Fe atoms (denoted

as Fe<sup>*b*</sup>). Therefore, as expected, the hybridization between the Fe<sup>*i*</sup>  $d$  and the Cr<sup>*i*</sup>  $d$  states for the  $m=3$  will not be as strong as that for  $m=1$ . It is interesting to note that the first nn environment of Fe<sup>*i*</sup> atoms for the

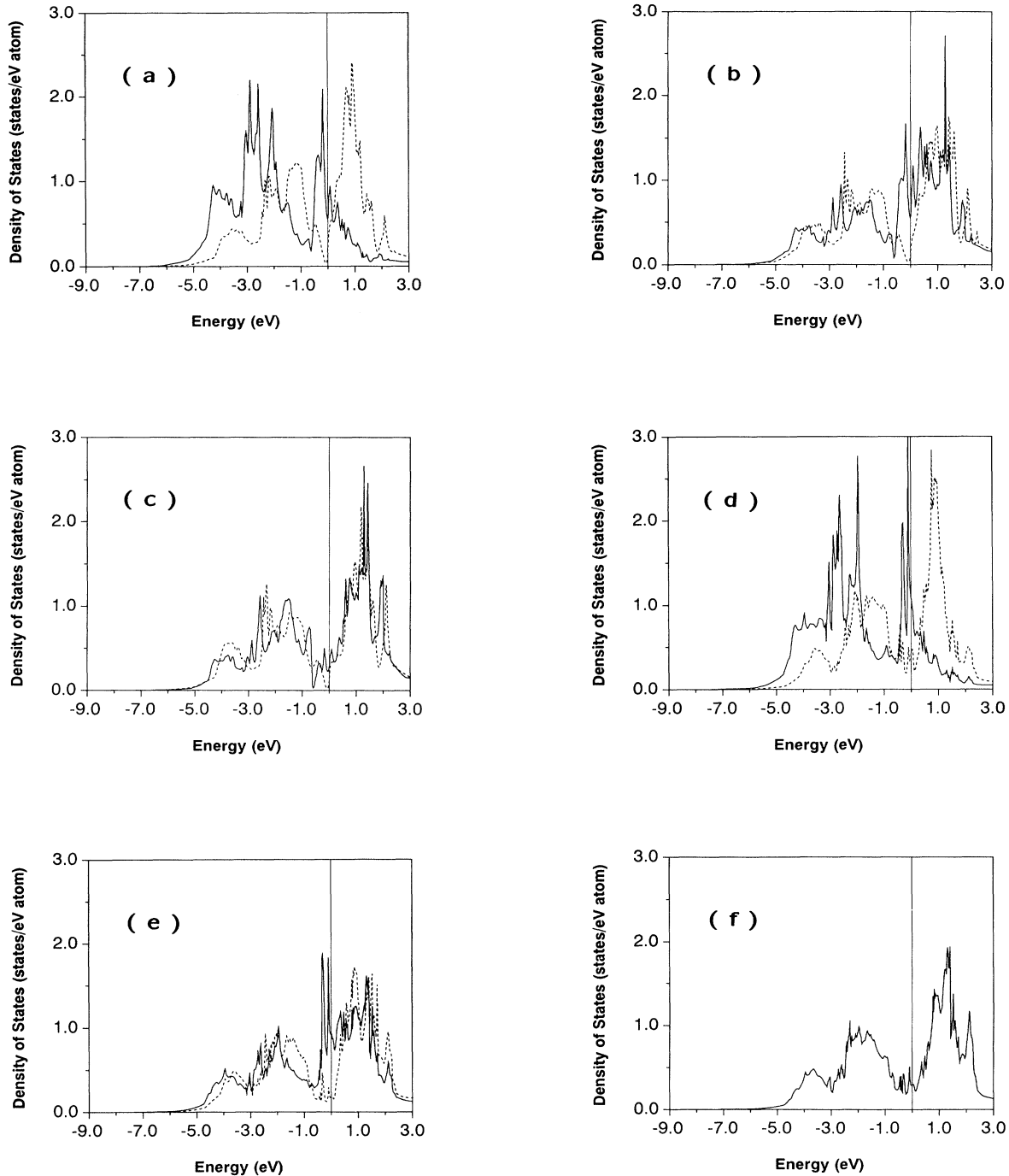


FIG. 5. Partial density of states (spin-polarized) for the Fe<sub>1</sub>/Cr<sub>3</sub>(001) superlattices in the FM configuration: (a) Fe<sup>*i*</sup>  $d$ , (b) Cr<sup>*i*</sup>  $d$ , and (c) Cr<sup>*b*</sup>  $d$  states, and in the AFM configuration; (d) Fe<sup>*i*</sup>  $d$ , (e) Cr<sup>*i*</sup>  $d$ , and (f) Cr<sup>*b*</sup>  $d$  states, only the partial DOS related with spin-up part on the Fe<sup>*i*</sup> sites is exhibited. Solid and dotted lines denote spin-up and spin-down states, respectively. Superscripts *i* and *b* stand for interface and bulklike atoms.

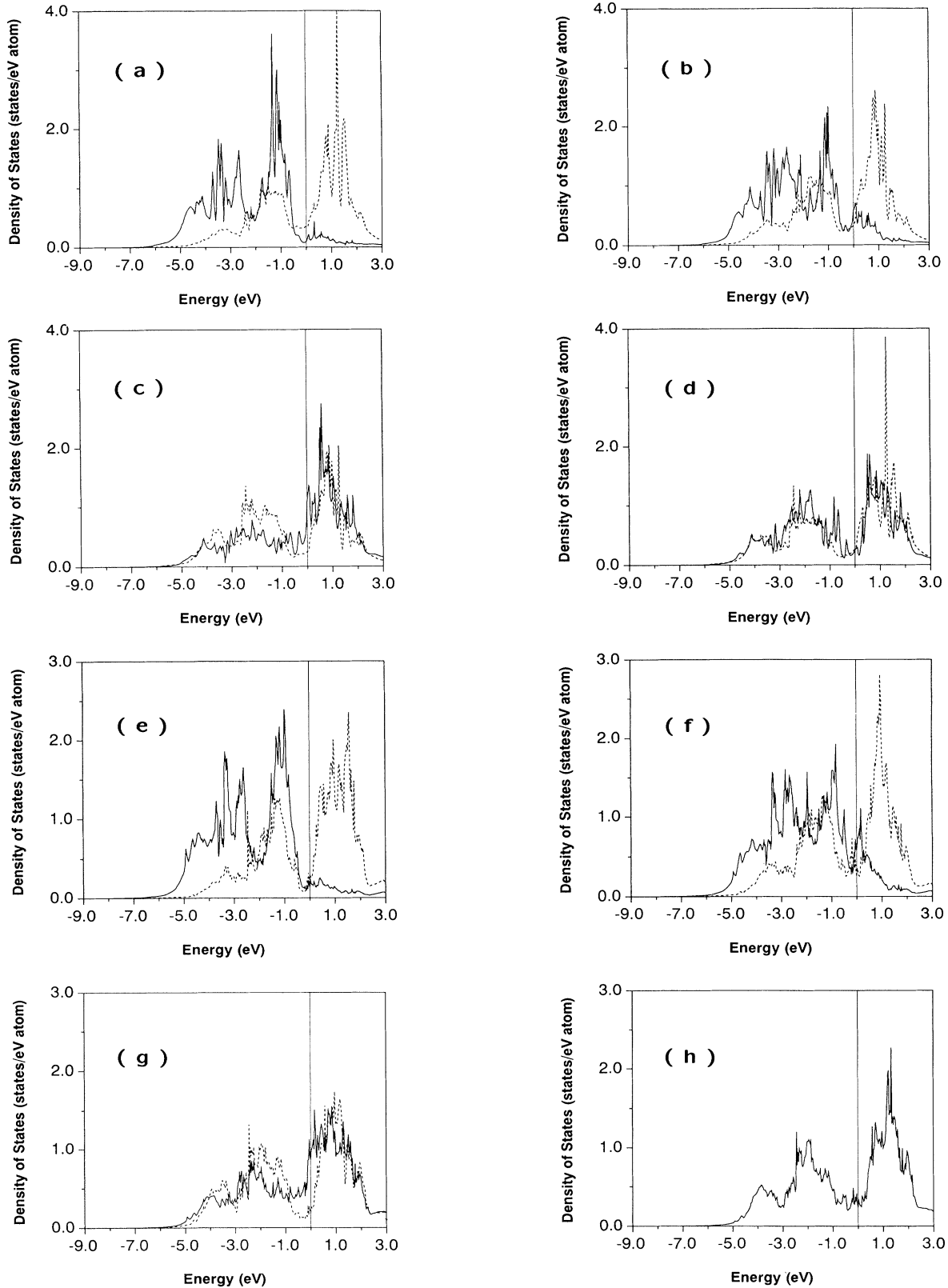


FIG. 6. Partial density of states (spin-polarized) for the  $\text{Fe}_3/\text{Cr}_3(001)$  superlattices in the FM configuration: (a)  $\text{Fe}^b d$ , (b)  $\text{Fe}^i d$ , (c)  $\text{Cr}^i d$ , and (d)  $\text{Cr}^b d$  states, and in the AFM configurations; (e)  $\text{Fe}^b d$ , (f)  $\text{Fe}^i d$ , (g)  $\text{Cr}^i d$ , and (h)  $\text{Cr}^b d$  states, only the partial DOS related with spin-up part on the  $\text{Fe}^b$  sites is exhibited. Solid and dotted lines denote spin-up and spin-down states, respectively. Super-scripts  $i$  and  $b$  stand for interface and bulklike atoms.

$\text{Fe}_m/\text{Cr}_n(001)$  ( $m=3$ ) superlattices is exactly same as that for the  $\text{Fe}_m/\text{Cr}_n(110)$  ( $m=1$ ) superlattices; this explains the resemblance of the  $d-d$  hybridization between these two systems and the same antiferromagnetic type Fe-Cr interlayer coupling.

#### ACKNOWLEDGMENTS

Work supported by the National Science Foundation DMR Grant No. 91-20521 and a grant from its Division for Advanced Scientific Computing at the Pittsburgh Supercomputing Center.

- 
- <sup>1</sup>M. N. Baibich, J. M. Broto, A. Fert, F. Nguyen Van dau, F. Petroff, P. Eitenne, G. Creuzet, A. Friederich and J. Chazelas, *Phys. Rev. Lett.* **61**, 2472 (1988); F. Nguyen Van Dau, A. Fert, P. Etienne, M. N. Baibich, J. N. Broto, J. Chazelas, G. Crenzet, A. Friederich, S. Hadjoudj, H. Hurdequint, J. P. Redoules, and J. Massies, *J. Phys. (Paris) Colloq.* **49**, C8-1633 (1988).
- <sup>2</sup>G. Binasch, P. Grunberg, F. Saurenbach, and W. Zinn, *Phys. Rev. B* **39**, 4828 (1989).
- <sup>3</sup>J. J. Krebs, P. Lubitz, A. Chaiken, and G. A. Prinz, *Phys. Rev. Lett.* **63**, 1645 (1989).
- <sup>4</sup>Teruya Shinjo, Satoru Araki, and Nobuyoshi Hosoito, *J. Magn. Magn. Mater.* **90**, & **91**, 753 (1990).
- <sup>5</sup>S. S. P. Parkin, N. More, and K. P. Roche, *Phys. Rev. Lett.* **64**, 2304 (1990).
- <sup>6</sup>P. M. Levy, K. Ounadjela, S. Zhang, Y. Wang, C. B. Sommers, and A. Fert, *J. Appl. Phys.* **67**, 5914 (1990).
- <sup>7</sup>Hideo Hasegawa, *Phys. Rev. B* **42**, 2368 (1990).
- <sup>8</sup>Daniel Stoeffler and Francois Gautier, *Prog. Theor. Phys. Suppl.* **101**, 139 (1990); K. Ounadjela, C. B. Sommers, A. Fert, D. Stoeffler, F. Gautier, and V. L. Moruzzi, *Europhys. Lett.* **15**, 875 (1991).
- <sup>9</sup>F. Herman, Juergen Sticht, and Mark Van Schilfgaarde, *J. Appl. Phys.* **69**, 4783 (1991).
- <sup>10</sup>Grunberg, S. Demokritov, A. Fuss, M. Vohl, and J. A. Wolf, *J. Appl. Phys.* **69**, 4789 (1991).
- <sup>11</sup>T. Jarlborg and A. J. Freeman, *J. Appl. Phys.* **53**, 8041 (1982).
- <sup>12</sup>N. Flevaris, Ph.D. thesis, Northwestern University, 1983.
- <sup>13</sup>J-h. Xu, A. J. Freeman, and T. Oguchi, *Bull. Am. Phys. Soc.* **32** (1987); *J. Magn. Magn. Mater.* **86**, 26 (1990).
- <sup>14</sup>O. K. Andersen, *Phys. Rev. B* **12**, 3060 (1975).
- <sup>15</sup>C. Sellers, Y. Shiroishi, N. K. Jaggi, J. B. Ketterson, and J. E. Hilliard, *J. Magn. Magn. Mater.* **54-57**, 787 (1986).
- <sup>16</sup>*Physical Metallurgy*, edited by R. W. Cahn and P. Haasen (North-Holland, Amsterdam, 1983), p. 178.
- <sup>17</sup>C. Kittel, *Introduction to Solid State Physics*, 5th ed. (Wiley, New York, 1976), p. 31.
- <sup>18</sup>U. von Barth and L. Hedin, *J. Phys. C* **5**, 1629 (1976).
- <sup>19</sup>F. Herman and P. Lambin, *J. Appl. Phys.* **57**, 3654 (1985).
- <sup>20</sup>E. Fawcett, *Rev. Mod. Phys.* **60**, 209 (1988).